Air Flow Distribution Analysis for APR1400 Integrated Head Assembly

Seonggi Jeong [a*], Kunwoo Yi [a], Byung Ryul Jung [a], Seok Jeong Yune [a], Seong Chan Park [a]
[a]*Fluid System Eng. Dep. NSSS Div. KEPCO E&C., 989-113 Daedeokdaero Yuseong-gu, Daejeon, Korea*
[*]*Corresponding author: seonggi@kepco-enc.com*

1. Introduction

.
The Integrated Head Assembly (IHA) is attached to the reactor vessel (RV) closure head. The IHA provides air flow path for cooling of control element drive mechanism (CEDM). CEDM cooling fans are located on the top of the IHA, which provide CEDM cooling air in the upper air plenum of IHA. The CEDM cooling system provides sufficient air flow to remove heat generated from the CEDM coils and the RV nozzles. The cooling system is provided to ensure that the CEDM cooling flows are within a required volumetric flow rate range.

This paper presents a CFD analysis of pressure drop and temperature distribution across each IHA air flow path and volumetric flow rate in each CEDM cooling shroud. It is important to cool CEDMs properly for integrity of CEDM operations. The analysis is aimed at checking the IHA cooling design data for CEDM cooling design.

2. Methods

APR1400 IHA geometry data is used for the analysis. The cooling air is introduced by fans that are located on the top of IHA and drawn off to the containment atmosphere.

2.1 Geometry data

A simplified IHA geometry is shown in Figure 1. The introduced cooling air through inlet ports provides CEDM cooling and goes down to the lower cooling shroud shell region to reject heat from RV nozzle. The heated air in the lower cooling shroud shell flows upward in four air baffles which direct air flow to the upper cooling shroud shell. The air flow baffles consist of two different flow areas. Discharged air from the baffles region gathers again in the upper cooling shroud shell and then is drawn off to the containment by the cooling fans. Three CEDM cooling fans are located on the top of the IHA.

Two cooling fans are operated at the normal operating condition and one cooling fan is standby. The CEDM cooling fans are operated with a shift operating method by the operators to minimize wearing out of one cooling fan more than the others. During the upset condition, the IHA can operate with a 50% increase in excess of the normal air flow.

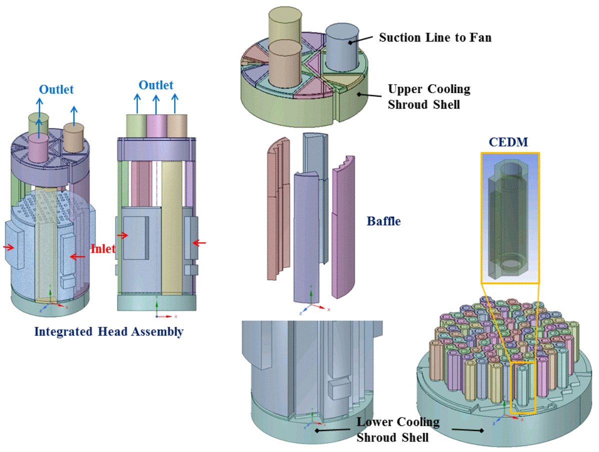

Fig. 1 Geometry for Integrated Head Assembly

2.2 Modeling

The analysis is performed using Fluent based on the finite volume method for turbulent, conjugate heat transfer simulation for incompressible and Navier-Stokes equations for Newtonian flow.

The k-ω SST turbulence model of Wilcox, Menter is used as the closure model for the turbulent flow in this analysis. The k-ω SST turbulence model is essentially the standard k-ω turbulence model in the fully turbulent region far from the wall and the k-ω turbulence model in the near wall region. A prism layers are used to flow boundary layers.

2.3 Input Data

Two air flow conditions are analyzed: Normal and Upset. Two fans are operating at normal condition and three fans are operating at upset condition. The cooling flow conditions are as follows;

- Normal condition: 1359.2 m^3/hr per CEDM,
- Upset condition: 2038.8 m^3/hr per CEDM.

Based on those cooling flow conditions, outlet velocity per cooling fan is calculated for input data. For each air flow condition, analysis is performed for the two containment air temperatures as follows;

- 15.5 ^{o}C ,
- 48.9 ^{o}C.

The properties of thermal conduction for the motor housing and RV nozzle are taken from ASME Section III Part D.

The used temperature distribution data for the Control Element Assembly (CEA) are calculated by considering heat transference from the RV nozzles and the motor housings. The applied inlet condition is at atmospheric pressure. The outlet condition is velocity and flow direction (Y-direction). Input data is summarized in Table I.

Table I. Input Data for Normal Condition & Upset Condition

	Condition I	Condition II
	Condition Ⅲ	Condition IV
Inlet Temperature [°C]	15.5	48.9
	15.5	48.9
Outlet Velocity per Cooling Fan [m/sec]	17.4	17.4
	17.4	17.4
Number of operating fan	2	2
	3	3

3. Results

3.1 Temperature distribution at CEDM and RV nozzle

The air temperature distribution around CEDM and RV nozzles is shown in Figure 2. The RV nozzle air temperature is higher than CEDM inlet temperature.

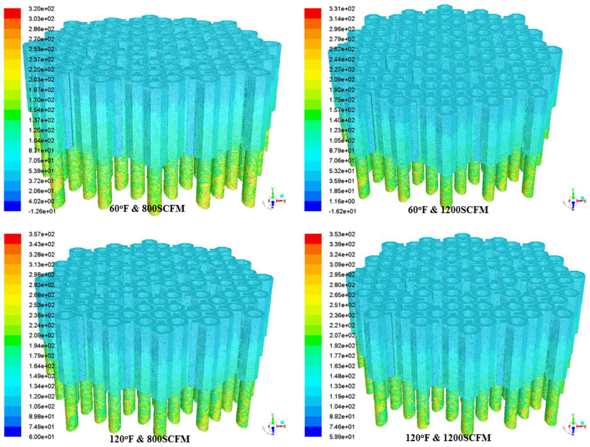

Fig. 2 Temperature distribution of IHA

The cooling air temperatures at two sections in the air flow path are summarized in Table II and Table III. It is shown that these temperatures at CEDM and baffle are in inversely proportional to flow rate of IHA.

A simplified temperature equation (1) derived from a law of conservation of mass and an ideal gas law can be used to check the CFD calculated temperatures.

$$\Delta T = c\frac{q}{\dot{m}\cdot C_p} = c'Q_S^{-1} \quad (1)$$

Table II. CEDM Temperature of IHA.

	CFD Analysis [°C]	Simplified Calculation [°C]
Condition I	35.8	25.1
Condition II	65.6	59.6
Condition Ⅲ	34.3	21.9
Condition Ⅳ	64.4	56.0

Table III. Baffle Temperature of IHA.

	CFD Analysis [°C]	Simplified Calculation [°C]
Condition I	48.7	34.9
Condition II	76.7	70.5
Condition Ⅲ	46.8	28.4
Condition Ⅳ	75.2	63.3

Calculated temperatures using the simplified temperature equation are higher than those obtained from CFD analysis. It is because constant specific heat values are used for the temperature equation. Also it is noted that the molecular contact forces is dependent on temperature Laplacian term of microscopic thermal energy equation.

3.2 Volumetric flow distribution across CEDM

Volumetric flow distribution across the CEDM is shown in Figure 3. It is noted that each volumetric flow shall fall within a required range for CEDM cooling as a design limit. The results show that volumetric flow for each CEDM falls within the required range.

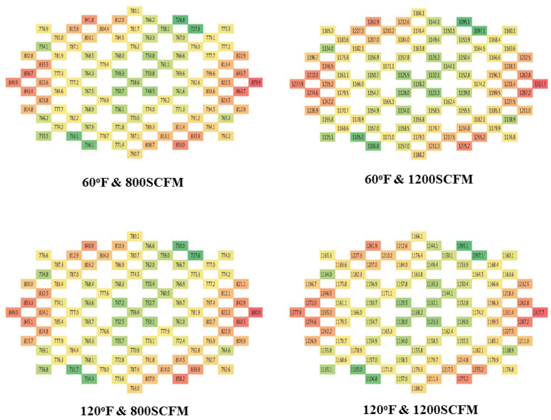

Fig. 3 Volumetric Flow Distribution across CEDM

3.3 Pressure drop along IHA Cooling Path

The pressure distributions are shown in Figure 4 and pressure drops along the IHA cooling paths are summarized in table IV for each analyzed condition.

Total pressure drops along the IHA cooling paths will depend on the air temperature at inlet and flow rate. The results show that the flow rate is more dominant than the air temperature in the calculated pressure drops.

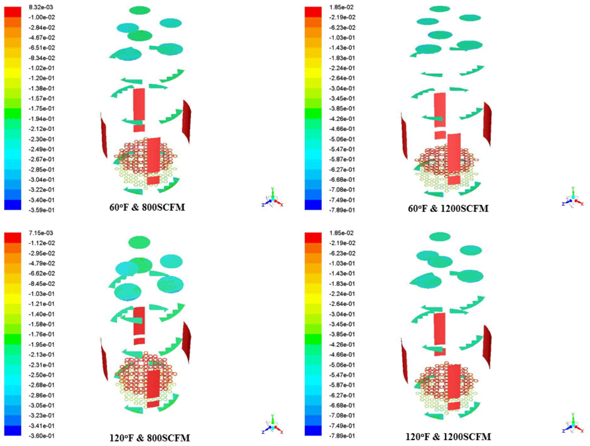

Fig. 4 Pressure Distribution of Integrated Head Assembly

Table IV. Pressure Drop of IHA at Each Condition.

	CFD Analysis [kPa]	Simplified Calculation [kPa]
Condition I	1.670	2.205
Condition II	1.697	2.461
Condition III	3.451	4.907
Condition IV	3.633	5.472

Since the cooling air is at atmospheric pressure at the inlet and if it is assumed that there will not be pressure change as much as $\Delta P/P > 10\%$, pressure drop can be calculated approximately from Darcy's formula.

$$\Delta P = cK \frac{Q_S^2}{T_R^{-1} A^2} \qquad (2)$$

From pressure drop equation (2), air temperature factors and flow rate factors are calculated by each condition data. The air temperature factor is about 4.35×10^{-3} and flow rate factor is about 2.25. Results of CFD analysis for pressure drop exactly match with temperature factor. On the other hand, flow rate factor is not matched with the CFD results. It is because the flow rate depends on temperatures at each section. It is noted that both factors are not much different and CFD pressure drops can be considered to be reasonable as a macroscopic analysis.

4. Conclusions

A comparison was performed between the CFD analysis and the simplified equation for IHA cooling in terms of temperature, flow distribution and pressure drop. The CFD analysis results showed a little difference to those calculated from a simplified equation. It is because the CFD analysis results are calculated by considering temperatures of IHA flow path as shown results. Finally both CFD and simplified equation showed as similar results as reasonably accepted in IHA cooling analysis.

REFERENCES

[1] Faith A. Morrison, An Introduction to Fluid Mechanics, Cambridge University Press, pp.429-493, 2013.

[2] ASME, 2015 ASEM Boiler & Pressure Vessel Code Section II Materials, ASME, Part D, 2015.

[3] CRANE, Flow of Fluids Through Valves, Fittings and Pipe Technical Paper No. 410, CRANE, Chapter 6, 2009.

[4] Wilcox D, Turbulence Modeling for CFD. 2nd Edition, DCW Industries, La Canada Flintridge, 1998.

[5] Versteeg H. and Malalasekera W. An Introduction to Computational Fluid Dynamics, Pearson Education Ltd, Harlow, 2007.